⌘ *Author's Choice*

THE JOURNAL OF BIOLOGICAL CHEMISTRY VOL. 286, NO. 16, pp. 13815–13826, April 22, 2011

Dual Role of CO_2/HCO_3^- Buffer in the Regulation of Intracellular pH of Three-dimensional Tumor Growths*[S]

Received for publication, January 16, 2011, and in revised form, February 15, 2011 Published, JBC Papers in Press, February 23, 2011, DOI 10.1074/jbc.M111.219899

Alzbeta Hulikova, Richard D. Vaughan-Jones, and Pawel Swietach[1]

From the Department of Physiology, Anatomy and Genetics, University of Oxford, Oxford OX1 3PT, United Kingdom

Intracellular pH (pH_i), a major modulator of cell function, is regulated by acid/base transport across membranes. Excess intracellular H^+ ions (*e.g.* produced by respiration) are extruded by transporters such as Na^+/H^+ exchange, or neutralized by HCO_3^- taken up by carriers such as Na^+-HCO_3^- cotransport. Using fluorescence pH_i imaging, we show that cancer-derived cell lines (colorectal HCT116 and HT29, breast MDA-MB-468, pancreatic MiaPaca2, and cervical HeLa) extrude acid by H^+ efflux and HCO_3^- influx, largely sensitive to dimethylamiloride and 4,4′-diisothiocyanatostilbene-2,2′-disulfonate (DIDS), respectively. The magnitude of HCO_3^- influx was comparable among the cell lines and may represent a constitutive element of tumor pH_i regulation. In contrast, H^+ efflux varied considerably (MDA-MB-468 > HCT116 > HT29 > MiaPaca2 > HeLa). When HCO_3^- flux was pharmacologically inhibited, acid extrusion in multicellular HT29 and HCT116 spheroids (~10,000 cells) was highly non-uniform and produced low pH_i at the core. With depth, acid extrusion became relatively more DIDS-sensitive because the low extracellular pH at the spheroid core inhibits H^+ flux more than HCO_3^- flux. HCO_3^- flux inhibition also decelerated HCT116 spheroid growth. In the absence of CO_2/HCO_3^-, acid extrusion by H^+ flux in HCT116 and MDA-MB-468 spheroids became highly non-uniform and inadequate at the core. This is because H^+ transporters require extracellular mobile pH buffers, such as CO_2/HCO_3^-, to overcome low H^+ ion mobility and chaperone H^+ ions away from cells. CO_2/HCO_3^- exerts a dual effect: as substrate for membrane-bound HCO_3^- transporters and as a mobile buffer for facilitating extracellular diffusion of H^+ ions extruded from cells. These processes can be augmented by carbonic anhydrase activity. We conclude that CO_2/HCO_3^- is important for maintaining uniformly alkaline pH_i in small, non-vascularized tumor growths and may be important for cancer disease progression.

Intracellular pH (pH_i)[2] is a permissive facilitator of growth and development in normal tissue and in tumors (1–3). Specialized proteins carry excess acid or base across membranes in a bid to maintain optimal pH_i. A major source of pH_i disturbance is cellular respiration, which loads cells with CO_2 or lactic acid. If uncompensated, these respiratory products ionize and acidify the intracellular milieu. Elevated metabolism in tumors predisposes cells to significant acid loading (4, 5), thus placing demand on mechanisms that regulate pH_i. The ability of tumors to maintain an alkaline pH_i (6) has been proposed as necessary for cancer progression (7). It is therefore of interest to study pH_i regulation in cancer, notably with respect to the characteristic features of tumor biology such as up-regulated glycolysis, acidic extracellular milieu, and aberrant vasculature (4, 5, 8).

Proteins that extrude H^+ ions have been the most intensively studied components of pH_i regulation in cancer. Na^+/H^+ exchangers (9–12) and V-type ATPase H^+ ion pumps (13, 14) are expressed in tumors and, at least under some conditions, have been linked to tumorigenesis through their role in pH_i regulation (1, 15, 16). Acid extrusion can also be produced by membrane transporters that load cells with HCO_3^- (or CO_3^{2-}) ions (17). These HCO_3^- transport proteins include electroneutral or 1:2 electrogenic Na^+-HCO_3^- cotransporters (NBC) (18–20) and Na^+-dependent Cl^-/HCO_3^- exchangers (21–23). Titration of intracellular acid with HCO_3^- produces CO_2, a soluble gas that exits through membranes passively to complete the acid extrusion process. For this component of pH_i regulation to function, cells must be supplied with CO_2/HCO_3^-, which *in vivo* is the principal extracellular pH buffer. Previous work on cancer cells has shown that HCO_3^- transport can alkalinize pH_i at normal and acidic extracellular pH (pH_e) (24) and contribute to pH_i recovery from acid loads (23, 25). However, a more complete characterization of HCO_3^- *versus* H^+ fluxes, in a range of cancer-derived cell lines at different values of pH_i and pH_e, has not been undertaken. Moreover, many studies of pH_i regulation have been carried out in the absence of CO_2/HCO_3^- buffer, *i.e.* under conditions where HCO_3^- transport is blocked.

For complete pH_i regulation at tissue level, the activity of membrane-bound acid extruders must be complemented with adequate diffusion of their transport solutes across the extracellular space. Accordingly, the rate of membrane HCO_3^- transport could be limited by diffusion of HCO_3^- toward cells and CO_2 diffusion in the opposite direction. Similarly, the activity of membrane-bound H^+ extruders must be complemented by efficient dissipation of the extracellularly deposited acid load; otherwise, extracellular acidification could slow the removal of cellular acid through a well documented inhibitory effect of extracellular H^+ ions on acid extruders (26, 27). In healthy tissue, plentiful blood perfusion helps to maintain the constancy

* This work was supported by grants from the Royal Society (to P. S.), Medical Research Council (to P. S.), and British Heart Foundation (to R. D. V.-J.).

[S] The on-line version of this article (available at http://www.jbc.org) contains supplemental Figs. S1–S7.

⌘ *Author's Choice*—Final version full access.

[1] To whom correspondence should be addressed: Dept. of Physiology, Anatomy and Genetics, Parks Rd., Oxford OX1 3PT, UK. E-mail: pawel.swietach@dpag.ox.ac.uk.

[2] The abbreviations used are: pH_i, intracellular pH; pH_e, extracellular pH; DMA, 5-(*N*,*N*-dimethyl)amiloride; DIDS, 4,4′-diisothiocyanatostilbene-2,2′-disulfonic acid; NHE, Na^+/H^+ exchangers; NBC, Na^+-HCO_3^- cotransporter(s); CA, carbonic anhydrase; ROI, region of interest.

and uniformity of extracellular pH, $[HCO_3^-]$, and $[CO_2]$. This, in turn, unifies pH_i regulation. In many solid tumors, however, perfusion tends to be heterogeneous, interrupted, and inadequate (5). This lengthens cell-to-capillary distances and weakens diffusive coupling across the extracellular space, particularly if this has high tortuosity (28). H^+ ions are, in addition, chemically reactive, and their binding to protonatable sites on large molecules, such as proteins, can impede free H^+ ion diffusion (29). It is therefore particularly important to ensure adequate mobility of extracellular H^+ ions. This can be achieved by the presence of mobile (*i.e.* diffusible) pH buffers. The diffusion of protonated buffer away from the site of H^+ ion production and the counter-flux of unprotonated buffer represent a form of facilitated H^+ ion diffusion. Although mobile buffers have been shown to facilitate H^+ ion diffusion inside cells (29–31), their role in facilitating extracellular H^+ ion mobility has not been studied in detail. A major extracellular mobile buffer is CO_2/HCO_3^-, but to evaluate its ability to facilitate H^+ ion diffusion, it is necessary to study multicellular growths that resemble tissue (*i.e.* harbor significant diffusion distances). Studies of pH_i regulation have, however, typically focused on biological processes occurring at the level of individual cells only.

Many cancer types have recently been linked with the expression of membrane-tethered, extracellular-facing carbonic anhydrase (CA) isoforms IX and XII (32, 33). The catalytic activity of these CA isoforms helps to maintain equilibrium between extracellular CO_2, HCO_3^-, and H^+ ions (34). The presence of these CAs in cancer tissue may be indicative of an important role for CO_2/HCO_3^- reactions in tumor pH_i regulation. In isolated cells, CA activity has been shown to accelerate the activity of membrane acid/base transporters (35–37) ("transport metabolon"). Within respiring spheroids, CAIX facilitates CO_2 removal from constituent cells (28, 38). It remains to be seen whether CA activity can support a role for CO_2/HCO_3^- in facilitating extracellular H^+ ion diffusion.

In the present work, we study the role of CO_2/HCO_3^- in pH_i regulation in a number of cancer-derived cell lines, prepared as single cells or as multicellular tissue-like growths (spheroids). We investigate the importance of CO_2/HCO_3^- as (i) a supply of substrate for acid-extruding HCO_3^- transporters and (ii) a mobile buffer supporting acid extrusion by facilitating extracellular H^+ ion diffusion. We show that HCO_3^- transport is an important component of pH_i regulation in all cell lines studied and that, in a number of cases, it can produce an acid extrusion flux that exceeds the capacity of H^+ transporters. In spheroids, we show that extracellular CO_2/HCO_3^- supports the activity of H^+ extruders by shuttling acid away from cells and minimizing the degree of extracellular acidification, which might otherwise inhibit membrane transport. Finally, we show that the effectiveness of CO_2/HCO_3^- as a mobile buffer is improved in the presence of CA activity. Our findings highlight an indispensable role of CO_2/HCO_3^- in tumor biology.

EXPERIMENTAL PROCEDURES

Cell Lines and Spheroid Culturing—Human colorectal carcinoma lines HCT116 and HT29 and the breast cancer cell line MDA-MB-468 were kind gifts from Professor Adrian Harris (Oxford, UK). The cervical carcinoma cell line HeLa was a kind gift from Professor Silvia Pastorekova (Bratislava, Slovakia). The pancreatic cell line MiaPaca2 was a kind gift from Professor Holger Kalthoff (Kiel, Germany). Cells were grown in Dulbecco's modified Eagle's medium (DMEM) containing $NaHCO_3$, in an atmosphere of 5% CO_2 for 48–72 h until 70–90% confluency was reached. Prior to experiments, cells were resuspended in Hepes-buffered DMEM (for up to 3 h), and aliquots of 200 μl were used for experiments. Spheroids were cultured using the hanging drop method (HCT116, 500 cells/20 μl; HT29, 1,000 cells/20 μl; MDA-MB-468, 5,000 cells/20 μl grown in 2.5% Matrigel) in HCO_3^- containing DMEM. For superfusion experiments, spheroids were grown for 2–3 days until they attained spherical symmetry and a radius of 130–200 μm (6,000–22,000 cells). To follow growth over a longer time frame, HCT116 spheroid formation and growth in hanging drops was extended to 4 days, after which spheroids were collected and transferred to non-tissue culture Petri dishes with HCO_3^--buffered DMEM media. This ensures that nutrient supply does not limit spheroid growth. Where desired, drugs were added to media before the onset of spheroid formation and throughout their growth, and compared with dimethyl sulfoxide (DMSO)-injected controls.

Confocal Imaging of pH—Single cells and spheroids were imaged using a Leica TCS NT confocal system and an IRBE microscope with a transparent superfusion chamber (capacity 2 ml), the base of which was pretreated with 0.01% poly-L-lysine to facilitate cell/spheroid adhesion. Solutions were heated to 37 °C and delivered at a constant rate (2 ml/min). Suction was adjusted to maintain a steady-state solution volume of ~0.5 ml. To measure intracellular pH, cells were loaded with the membrane-permeant acetoxymethyl ester of carboxy SNARF-1 (10 μM), a pH fluorophore, for 3 min (28). In the case of spheroids, loading time was extended to 30 min to allow adequate dye access to the core. Excess extracellular dye was washed away by superfusion. Carboxy SNARF-1 fluorescence, excited at 514 nm, was measured ratiometrically at 580 and 640 nm. To measure extracellular pH, spheroids were superfused with solution containing the membrane-impermeant pH fluorophore fluorescein-5-(and-6-)-sulfonic acid (30 μM) (28). Fluorescein-5-(and-6-)-sulfonic acid fluorescence, excited at 488 nm, was measured >510 nm.

Solutions, Drugs, and Superfusion Protocols—Cells and spheroids were superfused with solutions buffered by CO_2/HCO_3^- or Hepes. All solutions contained 4.5 mM KCl, 11 mM glucose, 1 mM $CaCl_2$, 1 mM $MgCl_2$. Hepes-buffered solutions contained 1–40 mM Hepes, and the pH of the solutions was adjusted with 4 M NaOH. CO_2/HCO_3^--buffered solutions were bubbled with either 5% CO_2/95% air or 20% CO_2/80% air and contained a concentration of $NaHCO_3^-$ that yielded the desired pH, in accordance with the Henderson-Hasselbalch equation ($pH = 10^{-6.15} + \log([HCO_3^-]/[CO_2])$). For all solutions, NaCl was added to produce a total osmolarity of 290–300 mosM/liter. In the case of Cl^--free solutions, all Cl^- salts were substituted with gluconates. All chemicals were obtained from Sigma-Aldrich (Poole, UK). Na^+/H^+ exchange was inhibited with 5-(*N*,*N*-dimethyl)amiloride (DMA; Sigma-Aldrich). HCO_3^- transport was inhibited with 4,4′-diisothiocyanatostilbene-

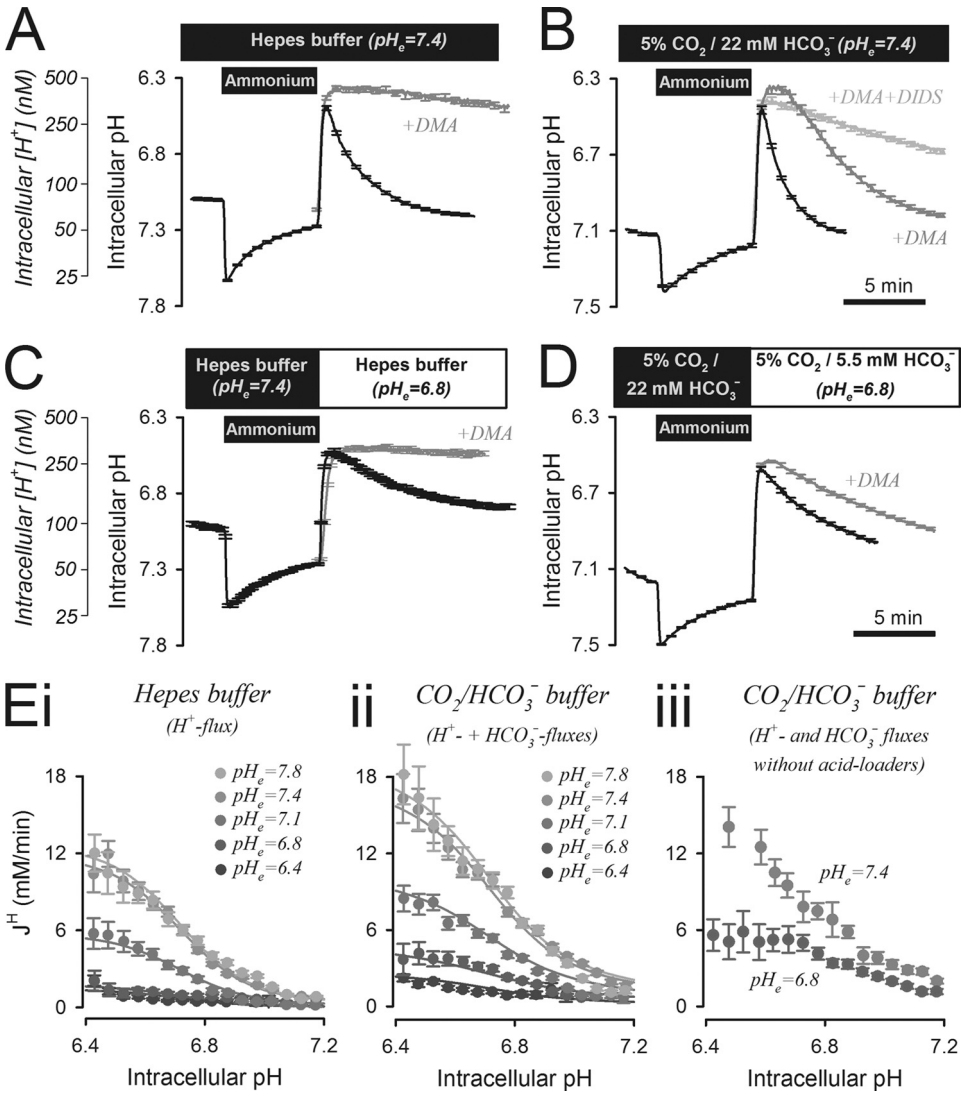

FIGURE 1. **Acid extrusion in isolated HCT116 cells.** *A*, ammonium prepulse (at $pH_e = 7.4$) performed to acid load HCT116 cells superfused with CO_2/HCO_3^--free, 20 mM Hepes buffer. pH_i recovery was inhibited by DMA (30 μM). Mean of >30 cells. *B*, ammonium prepulse (at $pH_e = 7.4$) performed to acid load HCT116 cells, superfused with 5% CO_2/22 mM HCO_3^- buffer. On removal of ammonium, pH_i recovery was partly inhibited by DMA (30 μM). The remainder of acid extrusion was sensitive to 300 μM DIDS. Mean of >30 cells. *C*, at the reduced pH_e of 6.8, pH_i recovery in Hepes buffer remained DMA-sensitive but was considerably slower than at $pH_e = 7.4$. *D*, in CO_2/HCO_3^- buffer, pH_i recovery was slower at low pH_e attained by reducing [HCO_3^-] to 5.5 mM. Mean of >30 cells. *E*, pH_i dependence of H^+ equivalent flux (J^H), measured over a range of pH_e and best-fitted to Hill equations describing activation by intracellular H^+ ions and inhibition by extracellular H^+ ions. *Panel I*, in Hepes buffer, showing H^+ flux; *panel ii*, in 5% CO_2 with varying [HCO_3^-], showing the sum of H^+ and HCO_3^- fluxes; *panel iii*, in 5% CO_2 and varying [HCO_3^-] in the absence of Cl^- (substituted with gluconate salts), showing acid extrusion fluxes in the absence of Cl^--dependent acid loaders. *Error bars* in all panels indicate S.E.

2,2′-disulfonic acid (DIDS; Sigma-Aldrich). Na^+-HCO_3^- cotransport was inhibited with S0859 kindly provided by Sanofi-Aventis (Frankfurt, Germany) (39). CA activity was blocked by acetazolamide (Sigma-Aldrich). The concentrations of DMA (30 μM), DIDS (150–300 μM), and S0859 (100 μM) used do not greatly affect membrane CA activity (supplemental Fig. S1). To produce an intracellular acid load, cells/spheroids were superfused with solution containing 20 mM NH_4Cl (less 20 mM NaCl) for 6 min. During exposure to ammonium, the intracellular compartment undergoes rapid alkalinization followed by gradual acidification arising from the activity of acid loaders. Removal of extracellular ammonium deposits an intracellular acid load that is subsequently removed by acid extruders, if active. Buffering (β) was measured using the ammonium removal method (supplemental Fig. S2) (40). Briefly, cells were exposed to a series of solutions of decreasing NH_4Cl concentrations that produce stepwise changes to pH_i. β was estimated from the ratio of the concentration of acid deposited in the cell during NH_4^+ withdrawal and the associated pH_i change.

RESULTS

Measuring the HCO_3^- Dependence and pH_i/pH_e Sensitivity of Acid Extrusion from Isolated Cells—Transmembrane extrusion of acid was first measured in single cells, using the time course of pH_i recovery from an intracellular acid load. Low pH_i was attained by an ammonium prepulse solution maneuver. Fig. 1*A* shows averaged pH_i time courses measured in carboxy SNARF-1-loaded HCT116 cells. Continuous superfusion ensured that the composition of the extracellular bathing medium was controlled. On removal of ammonium, pH_i decreased to a level that

stimulated acid extrusion. Recovery of pH_i in the absence of physiological CO_2/HCO_3^- buffer (replaced with Hepes) was mediated by HCO_3^--independent transport only. When pH_e was set to 7.4 (the pH of normal blood plasma), pH_i recovery was complete within 8 min. This was blocked by 30 μM DMA, indicating that Na^+/H^+ exchange (NHE) underlies the observed acid extrusion (27). In 5% CO_2/22 mM HCO_3^--buffered superfusates (Fig. 1*B*), pH_i recovery was accelerated and only partially blocked by DMA. The residual recovery was inhibited by DIDS, indicating that HCO_3^- transport contributes to pH_i regulation.

Acid extrusion from cells was quantified in terms of net H^+ equivalent flux (J^H), calculated as the product of the rate of pH_i change and intracellular buffering capacity ($J^H = -dpH_i/dt \times \beta$). This algorithm takes into account the vast concentration of H^+ ions held on buffers. Buffering capacity consists of a component due to intracellular CO_2/HCO_3^- (β_{carb}) and an "intrinsic" component (β_{int}) derived from membrane-impermeant intracellular buffers. β_{int} was measured in the absence of CO_2/HCO_3^- (supplemental Fig. S2, *A* and *B*) (40). Measurements in CO_2/HCO_3^--buffered superfusates yield the sum of β_{int} plus β_{carb} (supplemental Fig. S2, *C* and *D*). In 5% CO_2, measured β was equal to β_{int} plus an estimate of β_{carb} derived from the Henderson-Hasselbalch equation ($\beta_{carb} = 2.303\times[HCO_3^-]_e\times[H^+]_e/[H^+]_i$). The DMA-sensitive component of J^H measured in 5% CO_2/22 mM HCO_3^- was equal to the *total* J^H measured in the absence of CO_2/HCO_3^- (supplemental Fig. S4*A*). NHE activity in superfused single cells does not, therefore, require CO_2/HCO_3^- buffer. The DMA-insensitive component of J^H was inhibited by the broad spectrum HCO_3^- transport blocker DIDS or the Na^+-HCO_3^- cotransport blocker S0859 (supplemental Fig. S4*B*).

Acid extrusion in the absence of CO_2/HCO_3^- was reduced rapidly and reversibly at pH_e 6.8 (the typical pH_e of tumors (2, 41)), as expected from the inhibitory effect of extracellular H^+ ions on NHE (27) (Fig. 1*C*). Likewise, acid extrusion in the presence of CO_2/HCO_3^- buffer was also reduced at low pH_e, attained by dropping solution $[HCO_3^-]$ to 5.5 mM (a "metabolic acidosis"; Fig. 1*D*). Fig. 1*E*, *panels i* and *ii*, plot J^H as a function of pH_i and pH_e, measured in CO_2/HCO_3^--free and CO_2/HCO_3^--containing superfusates, respectively. For experiments in CO_2/HCO_3^-, pH_e was varied by changing $[HCO_3^-]$. HCO_3^- and H^+ fluxes increased as pH_i was reduced or as pH_e was raised. The decrease in J^H at low pH_e could be due to greater acid loading by transporters such as Cl^-/HCO_3^- exchange (42), rather than reduced activity of acid extruders. This was tested experimentally using solutions in which Cl^- salts were substituted with membrane-impermeant gluconates. Two sequential ammonium prepulses were performed to ensure that Cl^- had leaked out of cells. Fig. 1*E*, *panel iii* shows J^H measured in Cl^--free solutions after the second such ammonium prepulse. Solution pH was adjusted to 7.4 or 6.8 by varying $[HCO_3^-]$ at 5% CO_2. In the absence of Cl^--dependent acid loading, inhibition of J^H at low pH_e persisted, indicating that extracellular H^+ ions act in an inhibitory manner on acid extruders. A degree of activation of Cl^--driven acid loaders was, however, evident at $pH_e = 6.8$, but this was smaller than the inhibition of acid extrusion. In recognition of the modest activation of acid loaders at low pH_e, the process of pH_i recovery from an imposed acid load is referred to as *net* acid extrusion.

The metabolic acidosis attained by lowering solution $[HCO_3^-]$ may have reduced HCO_3^- flux because of rate-limiting substrate concentrations. To test this, recovery of pH_i was recorded in solutions that produce respiratory acidosis. Solution pH of 6.8 was attained by raising CO_2 partial pressure 4-fold at constant $[HCO_3^-]$ (supplemental Fig. S5*A*). This produced the same inhibitory effect on HCO_3^- flux as metabolic acidosis, suggesting that the activity of HCO_3^- transporters is instructed by extracellular $[H^+]$ rather than HCO_3^- availability.

Acid Extrusion by HCO_3^- Transport in Cancer-derived Cell Lines at Physiological and Acidic pH_e—In HCT116 cells superfused with 5% CO_2/22 mM HCO_3^- buffer, DIDS-sensitive HCO_3^- transport accounted for approximately one-third of total acid extrusion, whereas most of the remainder was due to DMA-sensitive H^+ transport (supplemental Fig. S4*B*). Acid extrusion was studied in four more cancer-derived cell lines: colorectal HT29, breast MDA-MB-468, pancreatic MiaPaca2, and cervical HeLa. Buffering capacity data for these cell lines are shown in supplemental Fig. S3. Membrane H^+ flux was calculated from pH_i recovery time courses measured in Hepes buffer titrated to 7.4 (Fig. 2*A*) or 6.8 (Fig. 2*B*). The additional HCO_3^- flux was estimated from pH_i recovery time courses in 5% CO_2/HCO_3^- buffer, with solution pH adjusted by varying $[HCO_3^-]$. At $pH_e = 7.4$, the magnitude of HCO_3^- flux was similar in all cell lines tested. When compared at a common pH_i of 6.7 (representing a modest intracellular acid load), HCO_3^- flux clustered at ~3.7 mM/min (from 3.0 mM/min in HeLa to ~4.3 mM/min in MDA-MB-468). In contrast, H^+ flux varied considerably, increasing in the order HeLa < MiaPaca2 < HT29 < HCT116 < MDA-MB-468, from 0.7 mM/min to 7.0 mM/min at $pH_i = 6.7$ (Fig. 2*A*). The mechanism of acid extrusion varied from predominantly HCO_3^- flux in HeLa, MiaPaca2, and HT29 to mainly H^+ flux in HCT116 and MDA-MB-468 cells. Nonetheless, HCO_3^- transport remained a significant component of pH_i regulation in all cell lines studied.

Extracellular acidification reduced HCO_3^- and H^+ fluxes (Fig. 2*B*). The pH_e sensitivity of these fluxes, probed at a common pH_i of 6.7, is shown in Fig. 2, *C* and *D*. Over the pH_e range studied, HCO_3^- flux was most pH_e-sensitive in MiaPaca2 cells and least pH_e-sensitive in HT29 cells. In contrast, HCT116 cells had the most pH_e-sensitive H^+ flux. Consequently, HCO_3^- flux in HCT116 cells became greater than H^+ flux over the pH_e range 7.05–6.4. The pH_e sensitivity of acid extrusion is important in the context of solid tumors, which are known to develop gradients of pH_e (2, 41) and hence are likely to show a depth dependence of transport phenotype. To address this, pH_i regulation was studied further in spheroids.

Spatial pH_i Regulation in Spheroids by Membrane HCO_3^- Flux—The ability of HCO_3^- transport to regulate pH_i in tissue-like structures was first investigated in spheroids composed of HT29 cells, a cell line in which acid extrusion relies principally on HCO_3^- flux (Fig. 2). The intracellular compartment of carboxy SNARF-1-loaded spheroids was acidified by means of an ammonium prepulse, and the subsequent pH_i recovery was monitored in 10 regions of interest (ROIs), defined as concentric rings within the boundary of the spheroid. To improve sig-

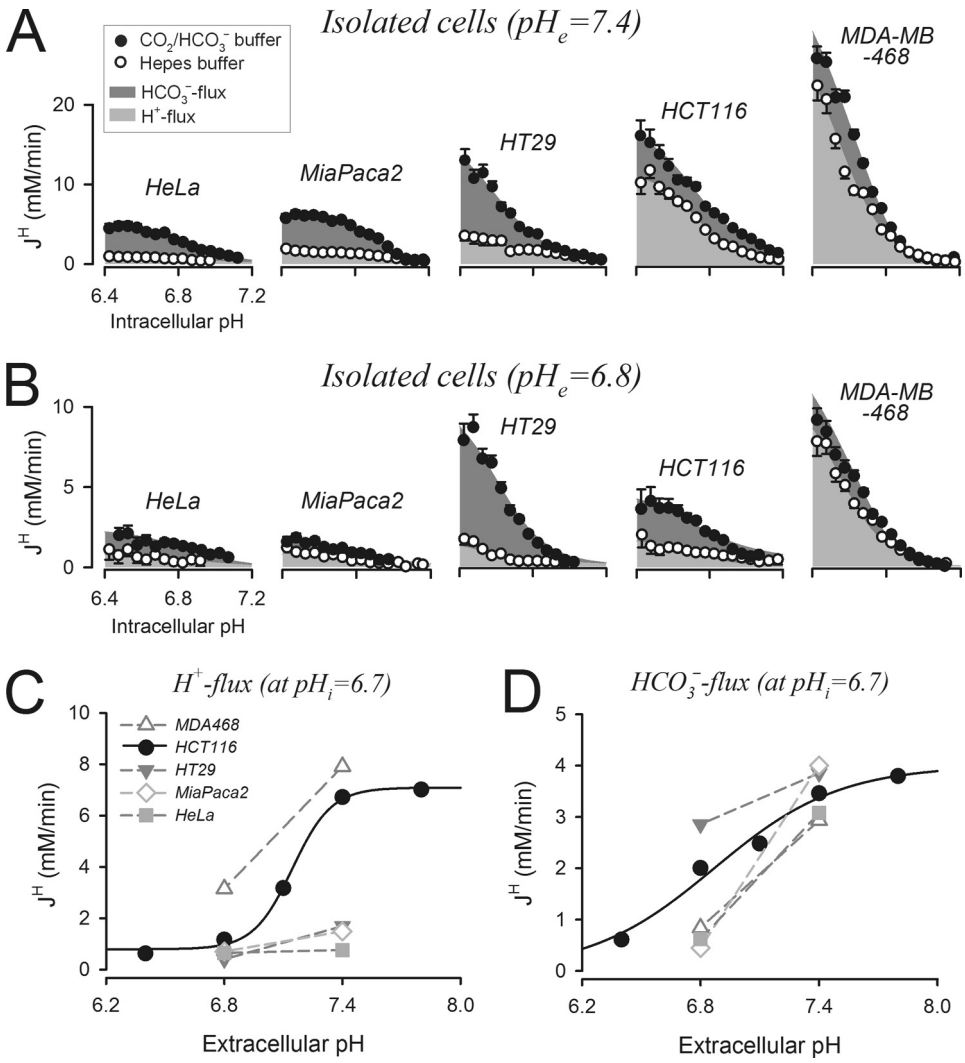

FIGURE 2. **Magnitude and pH_i/pH_e dependence of membrane H^+ and HCO_3^- fluxes in five cancer-derived lines.** *A*, pH_i dependence of H^+ flux (*light gray*) and HCO_3^- flux (*dark gray*), measured from pH_i recovery time courses at $pH_e = 7.4$, in the presence (*filled circles*) and absence (*open circles*) of CO_2/HCO_3^- buffer (mean of >30 cells). *B*, experiments repeated at $pH_e = 6.8$ (pH_e of CO_2/HCO_3^--buffered solutions adjusted by varying [HCO_3^-]). Mean cell radii (in μm): HeLa, 6.53 ± 0.07; MiaPaca2, 7.09 ± 0.08; HT29, 7.14 ± 0.11; HCT116, 6.55 ± 0.14; MDA-MB-468 7.11 ± 0.12. *Error bars* in *A* and *B* indicate S.E. *C*, pH_e sensitivity of H^+ flux probed at $pH_i = 6.7$. *D*, pH_e sensitivity of HCO_3^- flux probed at $pH_i = 6.7$.

nal-to-noise ratio, the four innermost ROIs were averaged (core). In CO_2/HCO_3^--buffered superfusates, pH_i recovery was complete within 8 min and proceeded fairly uniformly across the spheroid (Fig. 3*A*). In the presence of 150 μM DIDS, pH_i recovery was considerably slower and less uniform (Fig. 3*B*). The spheroid core remained acidic even after 12 min of pH_i recovery. Ammonium prepulse maneuvers in CO_2/HCO_3^- buffer were repeated on HCT116 spheroids. Recovery of pH_i from an acid load was fast and spatially coordinated, although a sizeable standing pH_i non-uniformity of 0.17 units persisted at steady state (2.5-fold greater than in HT29 spheroids). DIDS (300 μM) slowed pH_i recovery by 23% at periphery and 50% at core (Fig. 3*D*). The depth-dependent inhibitory effect of DIDS could be explained in terms of the pH_e gradient. With depth, pH_e is expected to fall (28, 43), and this, according to data in Fig. 2, would increase the share of HCO_3^- flux in overall acid extrusion in HT29 and HCT116 cells. Based on pH_e sensitivity, HCO_3^- flux is expected to produce more uniform pH_i recovery than H^+ flux. In support of this, acid extrusion in HCT116 spheroids was more uniform in the presence of DMA (30 μM; Fig. 3*E*) than in DIDS (Fig. 3*D*). To summarize, HCO_3^- transport in HT29 and HCT116 spheroids is important for spatially coordinated pH_i recovery from intracellular acid loads, particularly in deeper tissue regions.

The findings from colorectal cancer-derived spheroids show that HCO_3^- transport can play an important role in tissue pH_i regulation. To explore the effects of acid extrusion by H^+ transport and HCO_3^- transport on spheroid growth, the NHE inhibitor DMA or the NBC inhibitor S0859 was added to HCO_3^--buffered culture media incubated at 5% CO_2 (Fig. 3*F*). S0859 was used instead of DIDS to avoid nonspecific effects associated with stilbenes during exposures lasting several days. In the absence of NHE activity, spheroid growth ceased at a radius of 150 μm. In the absence of NBC activity, spheroid growth was reduced by 20–30%. The activity of NHE alone was not able to compensate for the absence of HCO_3^- transport in S0859. These results indicate that in HCT116 spheroids, pH_i-regulating fluxes via H^+ and HCO_3^- transporters are both important

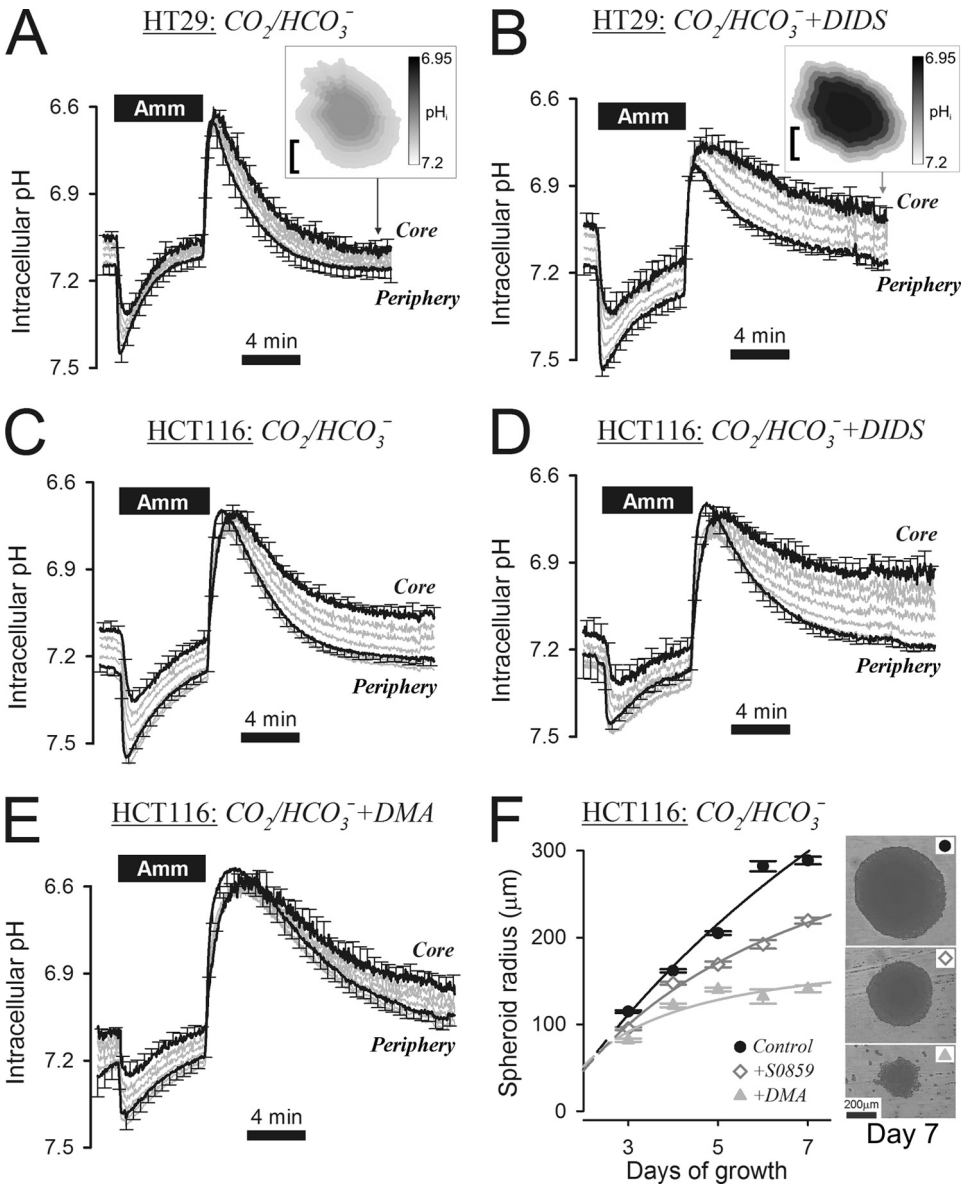

FIGURE 3. **HCO_3^- transport is important for uniform acid extrusion across HT29 and HCT116 spheroids.** *A*, 20 mM ammonium (*Amm*) prepulse performed on HT29 spheroid (mean radius 162.3 ± 10.8 μm). Bulk superfusate (pH = 7.4) was buffered by 5% CO_2/22 mM HCO_3^-. *Dark traces*: pH_i recovery at spheroid periphery (outer ROI) and core (mean of inner four ROIs). *Gray traces*: remaining ROIs. *Inset*: pH_i map (*bar* = 100 μm). End point pH_i gradient = 0.071 ± 0.023. *B*, experiment repeated in the presence of 150 μM DIDS to block HCO_3^- transport (mean spheroid radius = 182.6 ± 15.3 μm). *Inset*: pH_i map (*bar* = 100 μm). End point pH_i gradient = 0.180 ± 0.037. *C*, ammonium prepulse performed on HCT116 spheroid (mean radius 139.3 ± 6.2 μm). Bulk superfusate was buffered by 5% CO_2/22 mM HCO_3^- (pH = 7.4). End point pH_i gradient = 0.175 ± 0.049. *D*, experiment repeated in CO_2/HCO_3^- buffer in the presence of 300 μM DIDS to block HCO_3^- flux (mean spheroid radius = 129.7 ± 6.9 μm). Total flux inhibition at pH_i = 6.85 was 23% at the periphery and 50% at the core. End point pH_i gradient = 0.243 ± 0.059. *E*, experiment repeated in the presence of 30 μM DMA to block the major H^+ transporter, Na^+/H^+ exchange (mean spheroid radius = 141.8 ± 5.9 μm). Total flux inhibition at pH_i = 6.85 was 60% at the periphery and 50% at the core. End point pH_i gradient = 0.089 ± 0.067. *F*, HCT116 spheroid radius measured over 7 days in HCO_3^--containing media incubated in 5% CO_2. Growth curves were repeated in the presence of 30 μM DMA or 100 μM S0859 (HCO_3^- transport inhibitor) included before the onset of spheroid formation. Specimen images of day 7 spheroids are shown on the *right*. *Error bars* in all panels indicate S.E.

for tissue growth. This correlates with the additive ability of these transporters to alkalinize pH_i.

Facilitation of Membrane H^+ Flux by CO_2/HCO_3^- Buffer—H^+ transport was capable of producing significant, albeit non-uniform pH_i recovery in HCT116 spheroids (Fig. 3*D*). Acid extrusion by membrane H^+ flux was studied further in spheroids superfused with CO_2/HCO_3^--free, Hepes-buffered solutions (Fig. 4*A*). In the first set of experiments, pH_i recovery in 40 mM Hepes was similar to that measured in CO_2/HCO_3^- buffer in the presence of DIDS (Fig. 3*D*). This confirmed that DIDS-insensitive acid extrusion was active in Hepes-buffered superfusates. The addition of 30 μM DMA (supplemental Fig. S6) blocked pH_i recovery, identifying NHE as the major acid extruder. Hepes is not a physiological buffer; therefore further experiments were performed at lower Hepes concentrations: 10 mM (supplemental Fig. S7*A*) and 1 mM (Fig. 4*B*). As the concentration of buffer was reduced, pH_i recovery was slowed. This effect was most striking at the core, where diffusive coupling with the bulk superfusate was weakest. Further experiments were performed on spheroids cultured from MDA-MB-468

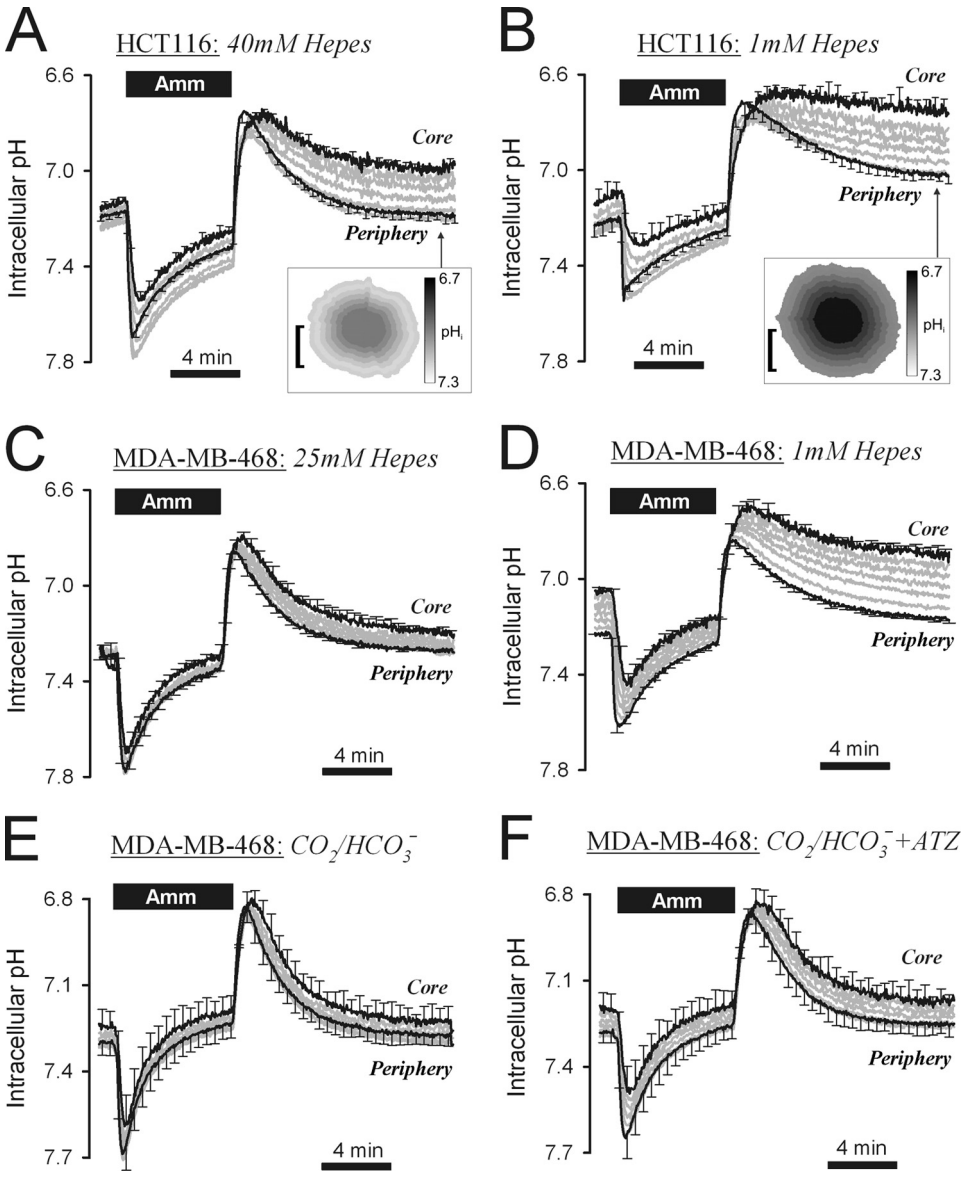

FIGURE 4. **Extracellular mobile buffers facilitate membrane H^+ transport in HCT116 and MDA-MB-468 spheroids.** *A*, 20 mM ammonium (*Amm*) prepulse performed on HCT116 spheroid (mean spheroid radius = 144.9 ± 8.7 μm), superfused with 40 mM Hepes-buffered solution at pH = 7.4. *Inset*: pH_i map (*bar* = 100 μm). End point pH_i gradient = 0.243 ± 0.044. *B*, experiment repeated with 1 mM Hepes-buffered solution at pH = 7.4 (mean radius 127.7 ± 3.9 μm). *Inset*: pH_i map (*bar* = 100 μm). End point pH_i gradient = 0.314 ± 0.079. *C*, ammonium prepulse performed on MDA-MB-468 spheroid (mean radius 127 ± 9.8 μm), superfused with 25 mM Hepes-buffered solution at pH = 7.4. End point pH_i gradient = 0.118 ± 0.008. *D*, experiment repeated in 1 mM Hepes-buffered solution. End point pH_i gradient = 0.284 ± 0.019. *E*, experiment repeated with superfusate buffered with 5% CO_2/22 mM HCO_3^- (mean radius 138 ± 13.0 μm). End point pH_i gradient = 0.051 ± 0.038. *F*, experiment continued in 100 μM acetazolamide (*ATZ*). End point pH_i gradient = 0.076 ± 0.039. Significant increase in pH_i at core ($p = 0.0052$) and periphery ($p = 0.0315$). *Error bars* in all panels indicate S.E.

cells, a cell line principally reliant on DMA-sensitive H^+ transport. At 25 mM Hepes, pH_i recovery was fast and fairly uniform (Fig. 4*C*). At 1 mM Hepes, pH_i recovery became significantly non-uniform and incomplete at the spheroid core, even after 12 min (Fig. 4*D*). By extrapolation, acid extrusion from the core of HCT116 and MDA-MB-468 spheroids would be expected to cease at 0 mM Hepes.

Adequate extracellular buffering is therefore necessary to support membrane H^+ transport. Blood contains CO_2/HCO_3^- that can provide pH buffering in lieu of Hepes. As shown in Fig. 3*D*, DIDS-insensitive H^+ transport in HCT116 spheroids was operational in CO_2/HCO_3^--buffered superfusates. Similarly, CO_2/HCO_3^- was able to substitute for Hepes in supporting membrane H^+ transport in MDA-MB-468 spheroids (Fig. 4*E*). These findings confirm the important role of CO_2/HCO_3^- buffer in facilitating acid extrusion from cells. To determine whether CA activity facilitates CO_2/HCO_3^- buffering, acid extrusion was studied in spheroids grown from MDA-MB-468 cells, a cell line showing significant hypoxic induction of CAIX (44). Inhibition of CA activity with acetazolamide reduced the rate of pH_i recovery by 15% at the spheroid periphery and 36% at the core, and yielded 50% greater pH_i non-uniformity (Fig. 4, *E* and *F*). These data suggest that the full potential of CO_2/HCO_3^- as a buffer requires CA activity.

In summary, the rate of net acid extrusion from cells within a spheroid is limited by the availability of extracellular mobile

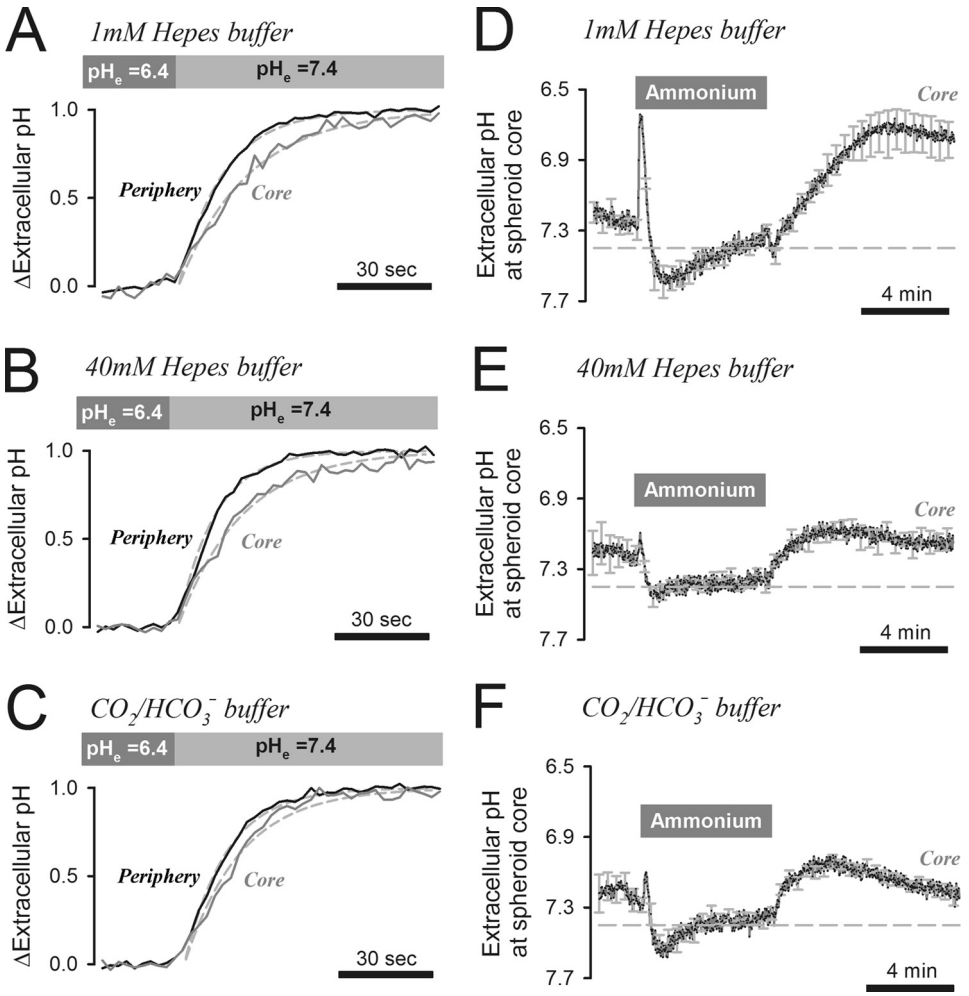

FIGURE 5. **Extracellular pH dynamics in HCT116 spheroids.** *A*, spheroid (mean radius 107 μm) pH$_e$, measured at the core and periphery ROIs (using the extracellular pH dye fluorescein-5-(and-6-)-sulfonic acid, included in all superfusates at 30 μM) during solution maneuvers switching bulk superfusate pH from 6.4 to 7.4. Bulk superfusate was buffered by 1 mM Hepes. Delay in pH$_e$ changes at the core and periphery of the spheroid gives an indication of the H^+ diffusion coefficient. *B*, experiment repeated in 40 mM Hepes. Mean spheroid radius = 109 μm. *C*, experiment repeated in 5% CO_2/22 mM HCO_3^- instead of Hepes. Mean spheroid radius = 92 μm. *D*, pH$_e$ measured at the core of spheroids during 20 mM ammonium prepulse. Bulk superfusate was buffered by 1 mM Hepes. *Inset*: pH$_e$ map (*bar* = 100 μm). *E*, experiment repeated with 40 mM Hepes. *F*, experiment repeated with 5% CO_2/22 mM HCO_3^-. The transient pH$_e$ acidification on the addition of ammonium is due to NH_4^+ deprotonation. Extracellular acidification following ammonium removal is due to the activation of acid extruders at low pH$_i$. *Error bars* in *D–F* indicate S.E.

buffering. It is noteworthy that this rate-limiting step for pH$_i$ regulation can only be studied in multicellular models, such as spheroids. In the diffusively restricted environment of tissue, extracellular acid can accumulate to levels that may modulate acid extrusion. Mobile buffers, such as Hepes and CO_2/HCO_3^-, can curtail the inhibitory effects of low pH$_e$ on acid extrusion (Fig. 2) by chaperoning extracellular H^+ ions away from the cell surface. This process was imaged in HCT116 spheroids using the membrane-impermeant pH$_e$ dye fluorescein-5-(and-6-)-sulfonic acid. Extracellular H^+ ion diffusion was driven by rapid switching between superfusates at pH 6.4 and 7.4 (Fig. 5, *A–C*). The delay of pH$_e$ change at the core of the spheroid, relative to its periphery, provided an estimate of the apparent extracellular H^+ ion diffusion coefficient (D_H^{app}). Periphery-to-core time delays were estimated from the time constants of exponentials best-fitted to the periphery and core time courses. These were then converted to D_H^{app} using a diffusion model with spherical symmetry (28). D_H^{app} estimates in superfusates buffered with 1, 10, and 40 mM Hepes were 137, 134, and 129 $\mu m^2/s$, respectively (Fig. 5, *A* and *B*; supplemental Fig. S7*B*). As explained under "Discussion," the lack of correlation between D_H^{app} and [Hepes] suggests that Hepes is the principal extracellular mobile buffer. In superfusates buffered with CO_2/HCO_3^-, the core delay was shorter and yielded a higher D_H^{app} of 211 $\mu m^2/s$ (Fig. 5*C*).

The diffusive flux of H^+ ions is given by the product of D_H^{app} and the concentration gradient of protonated buffer. Lower concentrations of buffer would therefore tend to produce smaller diffusive H^+ ion fluxes and allow greater pH$_e$ displacements during extrusion of cellular acid. Changes in pH$_e$ were investigated in HCT116 spheroids subjected to the ammonium prepulse maneuver in 1 mM, 40 mM Hepes (Fig. 5, *D* and *E*) or 5% CO_2/22 mM HCO_3^- (Fig. 5*F*). Exposure to ammonium produced an instantaneous and transient fall of pH$_e$ that was more pronounced under low buffering conditions (Fig. 5*D*). This pH$_e$ transient arises from NH_4^+ deprotonation driven by rapid NH_3 entry into cells (45). pH$_e$ transients in the opposite direction were observed on ammonium withdrawal under low buffering

only (Fig. 5*D*). On removal of ammonium, intracellular acidification of the spheroid stimulates acid extrusion, producing a more sustained reduction of pH_e. This reduction was large in 1 mM Hepes (Fig. 5*D*) but considerably smaller in 40 mM Hepes (Fig. 5*E*), presumably because diffusive H^+ flux was much greater under these latter conditions. The degree of acidification attained with 1 mM Hepes ($pH_e = 6.7$) is sufficient to attenuate H^+ efflux from cells and produce the degree of pH_i dispersion observed during pH_i recovery in Fig. 4, *B* and *D*. In the presence of CO_2/HCO_3^-, pH_e acidification is caused by H^+ efflux and HCO_3^- influx (Fig. 6, diagrams). CO_2/HCO_3^-, acting as a mobile buffer, was able to reduce the extent of pH_e acidification (Fig. 5*F*) and support further acid extrusion.

DISCUSSION

CO_2/HCO_3^- as a Source of Substrate for pH_i Regulating HCO_3^- Transport—Tumors require good pH_i control to support an intensive program of growth. The large metabolic acid loads deposited by elevated tumor metabolism emphasize the need for a pH_i regulatory system that remains functional even in tissue regions that are poorly perfused with blood. In all five cancer-derived cell lines tested, net acid extrusion is achieved by parallel pathways, one involving H^+ flux and another involving HCO_3^- flux. Despite awareness of HCO_3^- transporters in cancer, the latter flux has been largely ignored. H^+ and HCO_3^- fluxes can be quantified experimentally by measuring total acid extrusion fluxes in the presence and then absence of CO_2/HCO_3^- buffer, the substrate for HCO_3^- transport. These fluxes can also be dissected pharmacologically. Acid extrusion by H^+ transport is largely sensitive to DMA, a Na^+/H^+ exchanger inhibitor (Fig. 1*A*). The broad spectrum HCO_3^- transport inhibitor DIDS blocks most of the HCO_3^- flux (supplemental Fig.S4*B*). In HCT116 cells, HCO_3^- transport is sensitive to the Na^+-HCO_3^- cotransport inhibitor, S0859 (supplemental Fig. S4*B*) (39). Our preliminary data (not shown) provide evidence for NBCe1 expression in all five cell lines tested. However, S0859 is less potent on HT29 cells, indicating that the expression of different HCO_3^- transporters varies among cell lines.

The relative magnitude of H^+ and HCO_3^- fluxes varies with cell line, pH_i, and pH_e (Fig. 2). As expected from an effective homeostatic system for regulating pH_i, a rise in intracellular $[H^+]$ stimulates net acid extrusion in all five cell lines tested (Fig. 2). Allosteric activation of acid extruders by intracellular H^+ ions is likely to underlie this effect (26, 27). In contrast, a rise in *extracellular* $[H^+]$ inhibits acid extrusion (Fig. 2, *C* and *D*). This may represent a form of negative feedback that limits the degree of extracellular acidification. The share of the two acid extrusion mechanisms (*i.e.* H^+ *versus* HCO_3^- flux) forms a spectrum, ranging from mostly H^+ flux in MDA-MB-468 cells to largely HCO_3^- flux in HT29 or HeLa cells. In HT29 and HCT116 cells, unequal pH_e sensitivity of the two components of acid extrusion is responsible for the increase in the share of HCO_3^- transport as pH_e is reduced from 7.4 to 6.8. At $pH_e = 7.4$, H^+ flux varies by an order of magnitude, from very low in HeLa and MiaPaca2 to high in MDA-MB-468, and correlates with total J^H. Cell line-dependent variation in total J^H is therefore largely due to differences in H^+ flux. These differences do not correlate with cell radius, ranging narrowly from 6.53 ± 0.07 μm in HeLa to 7.14 ± 0.11 μm in HT29. Instead, variation in H^+ flux may arise from differences in transporter expression levels at the plasma membrane. In support of this, our preliminary data (not shown) provide evidence for higher expression of the mature (110-KDa) form of NHE1 in MDA-MB-468 and HCT116 cells, as compared with HeLa cells. It remains to be investigated whether, for example, variation in H^+ flux also correlates with respiratory rate or invasiveness. In contrast, similar levels of HCO_3^- flux are observed in all cell lines tested, suggesting that HCO_3^- transport may represent an essential and conserved element of tumor pH_i regulation.

Based on the present results, tumors with a pH_i regulation phenotype similar to HeLa or MiaPaca2 cells will rely on HCO_3^- transport for acid extrusion because of their low H^+ flux. Colorectal HT29 and HCT116 cell lines have a greater H^+ flux, yet when grown as spheroids, pH_i regulation at their core is driven largely by HCO_3^- flux (Fig. 3). The presence of DIDS produces non-uniform acid extrusion and increases core-to-periphery pH_i gradients (ΔpH_i), measured after 12 min of pH_i recovery, by 155% in HT29 spheroids and by 40% in HCT116 spheroids (Fig. 6*A*). HCO_3^- transport in these spheroids appears to be more capable of producing spatially unified pH_i regulation, as illustrated by the 2.7-fold smaller ΔpH_i measured in DMA in comparison with DIDS (Fig. 3, *D* and *E*). This arises because HCO_3^- transport in HT29 and HCT116 cells is less pH_e-sensitive than H^+ transport and more likely to persist at the acidic spheroid core. The shallow pH_e sensitivity of HCO_3^- flux may be a favorable adaptation in tumors that develop hypoxic cores yet require uniformly alkaline pH_i for coordinated growth. The deceleration of HCT116 spheroid growth in the presence of S0859 highlights the importance of HCO_3^- flux in cell proliferation (Fig. 3*F*) and the inability of residual H^+ flux to compensate for this.

CO_2/HCO_3^- as a Mobile Buffer Facilitating Extracellular Diffusion of Cell-extruded Acid—Regulation of pH_i has been viewed largely as a process involving acid/base transport across membranes, treating the cell as a self-contained entity. However, regulation of pH_i in tissue extends to acid/base fluxes across the extracellular space. This is illustrated by HCT116 and MDA-MB-468 spheroids, in which H^+ transporters cannot function efficiently without extracellular mobile buffers (Fig. 4). A number of tumors express high levels of H^+ transporters, akin to HCT116 and MDA-MB-468 cells. These transporters deposit H^+ ions into the extracellular space, where their mobility is restricted by the presence of protonatable sites on immobile buffer molecules, such as membrane-tethered proteins (29). In superfused single cells, solution flow is sufficient to wash away H^+ ions. However, in multicellular tissue, extracellular acidity may build up in poorly perfused spaces, thereby inhibiting further acid extrusion. In order for H^+ transporters to regulate pH_i, their activity must be complemented by facilitated H^+ ion diffusion across the extracellular space. Increasing the concentration of Hepes, a mobile buffer, accelerates acid extrusion in HCT116 and MDA-MB-468 spheroids (Fig. 4) by buffering the ensuing fall in pH_e (Fig. 5).

Physiologically, CO_2/HCO_3^- is the principal extracellular mobile buffer without which membrane H^+ transporters would not function to their full potential (Fig. 6*B*). In effect,

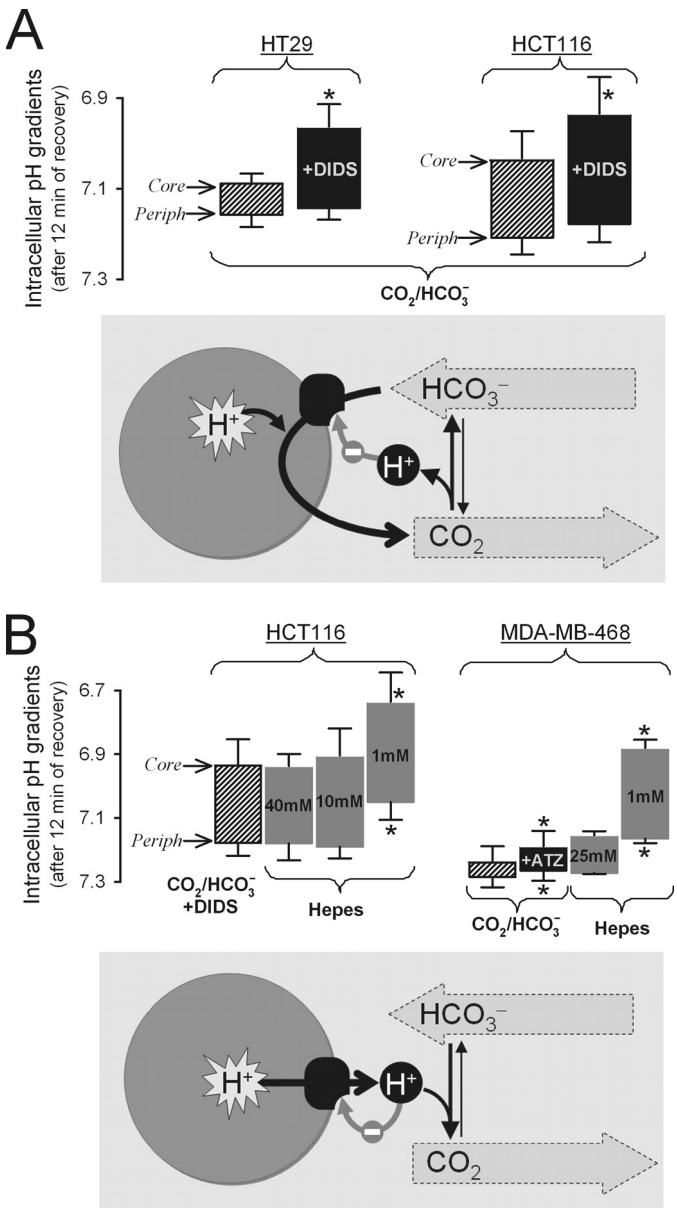

FIGURE 6. **Dual role of CO_2/HCO_3^- buffer in spatial pH_i regulation in tumor models.** Histograms show the pH_i gradient from the spheroid core (*upper edge of histogram bar*) to its periphery (*Periph*, *lower edge*) measured after 12 min of recovery from an imposed acid load. *Asterisks* denote statistically significant differences as compared with control (*shaded bars*) at the 5% level using unpaired Student's *t* tests, except for testing the effects of acetazolamide (*ATZ*), where paired Student's *t* tests were performed. *Error bars* in both panels indicate S.E. *A*, the importance of membrane HCO_3^- transport in spheroids bathed in 5% CO_2/22 mM HCO_3^- buffer (data from Fig. 3). In HT29 and HCT116 spheroids treated with the HCO_3^- transport inhibitor DIDS, core pH_i was more acidic than control, and hence core-to-periphery pH_i gradients increased. This indicates that HCO_3^- transport is particularly important for regulating pH_i at the spheroid core, thereby ensuring uniform pH_i control throughout the spheroid. The diagram (*lower panel*) illustrates the role of HCO_3^- transport in acid extrusion. The *thin gray arrow* represents negative feedback on net acid extrusion. *B*, the importance of mobile buffers in facilitating H^+ extrusion in HCT116 and MDA-MB-468 spheroids. Core-to-periphery pH_i gradients were measured in media buffered by 5% CO_2/22 mM HCO_3^- or Hepes (data from Figs. 3 and 4). HCT116 spheroids bathed in CO_2/HCO_3^- were treated with DIDS to ensure that the principal process driving acid extrusion was H^+ efflux. pH_i gradients increased as extracellular Hepes concentration was decreased. Mobile buffering provided by 5% CO_2/22 mM HCO_3^- was equivalent to ~30 mM Hepes. In CO_2/HCO_3^- buffer, inhibition of CA activity with acetazolamide (*ATZ*) slowed pH_i recovery and increased pH_i non-uniformity. These results indicate that CO_2/HCO_3^-, by acting as a mobile buffer, facilitates acid extrusion throughout the spheroid and helps to attain more uniform pH_i control. The diagram (*lower panel*) illustrates the role of CO_2/HCO_3^-, the physiological extracellular mobile pH buffer, in spatial pH_i regulation. The *thin gray arrow* represents negative feedback on net acid extrusion.

even nominally HCO_3^--independent H^+ transporters, such as NHE, require extracellular CO_2/HCO_3^-. This observation emphasizes the need to provide physiologically relevant mobile buffering in studies of pH_i regulation in multicellular tissue. In CO_2/HCO_3^--free superfusates, two pieces of evidence point to the absence of intrinsic mobile buffering within the spheroid extracellular compartment. Firstly, by extrapolating pH_i recovery time courses to zero [Hepes] (Fig. 4), acid extrusion from spheroid cores is predicted to cease. Secondly, the apparent H^+ ion diffusion coefficient (D_H^{app}) is independent of [Hepes] over the 1–40 mM range (Fig. 5). D_H^{app} is a mean of the diffusion coefficients (D) of all participating buffers, weighted by buffering capacity (β).

$$D_H^{app} = (D_1 \cdot \beta_1 + \ldots + D_n \cdot \beta_n)/(\beta_1 + \ldots + \beta_n) \quad \text{(Eq. 1)}$$

However, as [Hepes], and hence its β, is reduced, measured D_H^{app} does not change. This indicates that even at 1 mM, Hepes is the principal extracellular buffer. Tumors *in situ* may, however, regulate D_H^{app} by secreting mobile buffers yet to be characterized.

By comparing pH_i gradient data from Fig. 6*B*, 5% CO_2/22 mM HCO_3^- can be interpolated to have a mobile buffer capacity equivalent to ~30 mM Hepes, *i.e.* higher mole-for-mole, partly because of its smaller size and hence higher diffusion coefficient (Fig. 5). The ability of CO_2/HCO_3^- to facilitate H^+ ion diffusion can be limited by its inherently slow reaction kinetics, in particular CO_2 hydration (34). This limiting factor could be eliminated by expressing cancer-related extracellular CAs, which catalyze CO_2-HCO_3^- interconversion. Indeed, CA inhibition with acetazolamide reduces the rate of acid extrusion in MDA-MB-468 spheroids and increases ΔpH_i by 50% (Fig. 6*B*). CA activity can therefore accelerate membrane H^+ flux, most likely by increasing the effective buffering capacity provided by CO_2/HCO_3^-. Because a membrane-permeant inhibitor was used, it could be argued that inhibition of intracellular CA activity underlies the acetazolamide effect. However, the effect of CA inhibition increases with spheroid depth, suggesting that CA accelerates a process that is distance-dependent, such as extracellular diffusion (34). Any such effect would add to previously described interactions of H^+ transporters with intracellular CAs (35).

Spheroids as Models of Developing Tumors—Studies of single superfused cells cannot adequately describe pH_i regulation in cancer tissue because of the multicellular nature and suboptimal perfusion of tumors. Spheroids, like growing tumors, harbor a restricted extracellular space in which cell-extruded H^+ ions may accumulate. In addition, spheroids can be imaged for pH_i and pH_e, and the composition of their extracellular space can be manipulated through the bulk superfusate (28, 38). The radii of spheroids (~150 μm) imaged in the present work mimic the diffusion distances that are characteristic of the viable rim in tumors (46), which does not develop severe hypoxia (48). Larger spheroids were not studied in order to limit the

development of hypoxia that could *per se* affect acid extrusion significantly (47). It is plausible that modest hypoxia, acting via gene regulation or energy supply, could have contributed to the slowing of pH_i recovery at the core of spheroids. Maneuvers such as changing extracellular buffering capacity or inhibiting acid/base transport are not expected to alter O_2 gradients, so by pairing experiments with controls, it should be possible to account for any background effects of hypoxia.

Superfusates buffered by 5% CO_2/22 mM HCO_3^- mimic blood plasma. Within the spheroid extracellular space, the composition of this buffer is likely to change in a manner that reflects the tumor microenvironment, *i.e.* low pH_e, cellular CO_2 production, and HCO_3^- transport across membranes. Thus, CO_2/HCO_3^--dependent buffering established within spheroids is likely to attain a magnitude that is relevant to developing tumors. The low pH_e in tumors is usually associated with low HCO_3^- concentrations. For instance, as pH_e is dropped from 7.4 to 6.8 at constant CO_2 partial pressure, equilibrium [HCO_3^-] falls 4-fold. Such a fall in extracellular [HCO_3^-] is not rate-limiting for HCO_3^- flux, at least in HCT116 cells, as measurements at pH_e 6.8 with 22 mM and 5.5 mM HCO_3^- yield the same acid flux (supplemental Fig. S5). With such high affinity for HCO_3^-, even low millimolar concentrations of HCO_3^- may suffice for HCO_3^--driven acid extrusion.

CO_2/HCO_3^- and Cancer—The flux diagrams in Fig. 6 summarize the two roles of CO_2/HCO_3^- in pH_i regulation. These fluxes are ultimately powered by active membrane transport. However, without CO_2/HCO_3^-, they would cease to operate because of the lack of transporter substrate (Fig. 6*A*) or inadequate dissipation of extruded H^+ ions (Fig. 6*B*). The dominance of either pathway will depend on the relative magnitude of transmembrane H^+ and HCO_3^- fluxes during acid extrusion. As shown in the present work, the balance between H^+ and HCO_3^- fluxes varies with cell line and therefore cancer type. Moreover, the share of these fluxes may vary regionally within a solid tumor due to the action of modulators, including pH_e.

A notable difference in the two schemes is the relationship between extracellular H^+ ions and CO_2/HCO_3^-. Under the first scheme (Fig. 6*A*), cellular uptake of HCO_3^- in exchange for CO_2 produces an out-of-equilibrium state that drives H^+ release from CO_2, particularly in the presence of extracellular CAs (51). In contrast, under the second scheme (Fig. 6*B*), CO_2/HCO_3^- buffer takes up a fraction of cell-extruded H^+ ions. At steady state, the two schemes will converge at an acidic pH_e, a hallmark of cancer that is believed to exert selection pressure against normal cells and promote tumor invasiveness (7, 8). Inhibition of H^+ and HCO_3^- fluxes at very low pH_e would, however, serve as a feedback mechanism to prevent excessive extracellular acidification (Fig. 6). Buffering of extracellular acidity with plasma HCO_3^- supplementation has been proposed as a novel means of combating tumors (49). The effectiveness of such treatment will have to be weighed against the beneficial effect of raised HCO_3^- on pH_i control in tumor cells.

The present work highlights the importance of CO_2/HCO_3^- for coordinating pH_i regulation spatially. Non-uniformity of acid extrusion will tend to produce spatially heterogeneous steady-state pH_i, which may lead to poor coordination of tissue growth and function. Unlike normal tissue, cancer cannot rely on blood flow to unify pH_e or gap junctions to synchronize pH_i because perfusion tends to be heterogeneous, interrupted, and inadequate (5) and gap junction proteins are typically absent (50). Expression of HCO_3^- transporter isoforms, particularly of low pH_e sensitivity, plus extracellular carbonic anhydrases to keep CO_2/HCO_3^- buffer at equilibrium may be a compensatory means of improving spatial pH_i regulation by exploiting the dual role of CO_2/HCO_3^- buffer. Proteins implicated in CO_2/HCO_3^- reactions and transport may improve tumor survival and may therefore be targets for therapy.

Acknowledgments—We thank Professor Adrian Harris for valuable discussions. S0859 was kindly provided by Dr. Heinz-Werner Kleemann (Sanofi-Aventis).

REFERENCES

1. Pouysségur, J., Sardet, C., Franchi, A., L'Allemain, G., and Paris, S. (1984) *Proc. Natl. Acad. Sci. U.S.A.* **81,** 4833–4837
2. Chiche, J., Brahimi-Horn, M. C., and Pouysségur, J. (2010) *J. Cell. Mol. Med.* **14,** 771–794
3. Boron, W. F. (2004) *Adv. Physiol. Educ.* **28,** 160–179
4. Gatenby, R. A., Gawlinski, E. T., Gmitro, A. F., Kaylor, B., and Gillies, R. J. (2006) *Cancer Res.* **66,** 5216–5223
5. Vaupel, P., Kallinowski, F., and Okunieff, P. (1989) *Cancer Res.* **49,** 6449–6465
6. Gillies, R. J., Raghunand, N., Garcia-Martin, M. L., and Gatenby, R. A. (2004) *IEEE Eng. Med. Biol. Mag.* **23,** 57–64
7. Fang, J. S., Gillies, R. D., and Gatenby, R. A. (2008) *Semin. Cancer Biol.* **18,** 330–337
8. Gatenby, R. A., and Gillies, R. J. (2004) *Nat. Rev. Cancer* **4,** 891–899
9. Orlowski, J., and Grinstein, S. (2004) *Pflugers Arch.* **447,** 549–565
10. Murer, H., Hopfer, U., and Kinne, R. (1976) *Biochem. J.* **154,** 597–604
11. Sardet, C., Franchi, A., and Pouysségur, J. (1989) *Cell* **56,** 271–280
12. Orlowski, J., Kandasamy, R. A., and Shull, G. E. (1992) *J. Biol. Chem.* **267,** 9331–9339
13. Pedersen, P. L., and Carafoli, E. (1987) *Trends Biochem. Sci.* **12,** 146–150
14. Martinez-Zaguilan, R., Lynch, R. M., Martinez, G. M., and Gillies, R. J. (1993) *Am. J. Physiol.* **265,** C1015–C1029
15. Reshkin, S. J., Bellizzi, A., Caldeira, S., Albarani, V., Malanchi, I., Poignee, M., Alunni-Fabbroni, M., Casavola, V., and Tommasino, M. (2000) *FASEB J.* **14,** 2185–2197
16. Gillies, R. J., Martinez-Zaguilan, R., Martinez, G. M., Serrano, R., and Perona, R. (1990) *Proc. Natl. Acad. Sci. U.S.A.* **87,** 7414–7418
17. Boron, W. F., and Boulpaep, E. L. (1983) *J. Gen. Physiol.* **81,** 53–94
18. Deitmer, J. W., and Schlue, W. R. (1989) *J. Physiol.* **411,** 179–194
19. Choi, I., Aalkjaer, C., Boulpaep, E. L., and Boron, W. F. (2000) *Nature* **405,** 571–575
20. Romero, M. F., Hediger, M. A., Boulpaep, E. L., and Boron, W. F. (1997) *Nature* **387,** 409–413
21. Wang, C. Z., Yano, H., Nagashima, K., and Seino, S. (2000) *J. Biol. Chem.* **275,** 35486–35490
22. Romero, M. F., Henry, D., Nelson, S., Harte, P. J., Dillon, A. K., and Sciortino, C. M. (2000) *J. Biol. Chem.* **275,** 24552–24559
23. Wong, P., Kleemann, H. W., and Tannock, I. F. (2002) *Br. J. Cancer* **87,** 238–245
24. Lee, A. H., and Tannock, I. F. (1998) *Cancer Res.* **58,** 1901–1908
25. Lauritzen, G., Jensen, M. B., Boedtkjer, E., Dybboe, R., Aalkjaer, C., Nylandsted, J., and Pedersen, S. F. (2010) *Exp. Cell Res.* **316,** 2538–2553
26. Vaughan-Jones, R. D., and Wu, M. L. (1990) *J. Physiol.* **428,** 441–466
27. Aronson, P. S. (1985) *Annu. Rev. Physiol.* **47,** 545–560
28. Swietach, P., Patiar, S., Supuran, C. T., Harris, A. L., and Vaughan-Jones, R. D. (2009) *J. Biol. Chem.* **284,** 20299–20310
29. Irving, M., Maylie, J., Sizto, N. L., and Chandler, W. K. (1990) *Biophys. J.* **57,** 717–721

30. Vaughan-Jones, R. D., Peercy, B. E., Keener, J. P., and Spitzer, K. W. (2002) *J. Physiol.* **541,** 139–158
31. Stewart, A. K., Boyd, C. A., and Vaughan-Jones, R. D. (1999) *J. Physiol.* **516,** 209–217
32. Pastorek, J., Pastoreková, S., Callebaut, I., Mornon, J. P., Zelník, V., Opavský, R., Zat'ovicová, M., Liao, S., Portetelle, D., and Stanbridge, E. J. (1994) *Oncogene* **9,** 2877–2888
33. Türeci, O., Sahin, U., Vollmar, E., Siemer, S., Göttert, E., Seitz, G., Parkkila, A. K., Shah, G. N., Grubb, J. H., Pfreundschuh, M., and Sly, W. S. (1998) *Proc. Natl. Acad. Sci. U.S.A.* **95,** 7608–7613
34. Swietach, P., Hulikova, A., Vaughan-Jones, R. D., and Harris, A. L. (2010) *Oncogene* **29,** 6509–6521
35. Li, X., Alvarez, B., Casey, J. R., Reithmeier, R. A., and Fliegel, L. (2002) *J. Biol. Chem.* **277,** 36085–36091
36. Sterling, D., Reithmeier, R. A., and Casey, J. R. (2001) *J. Biol. Chem.* **276,** 47886–47894
37. Morgan, P. E., Pastoreková, S., Stuart-Tilley, A. K., Alper, S. L., and Casey, J. R. (2007) *Am. J. Physiol. Cell Physiol.* **293,** C738–C748
38. Swietach, P., Wigfield, S., Cobden, P., Supuran, C. T., Harris, A. L., and Vaughan-Jones, R. D. (2008) *J. Biol. Chem.* **283,** 20473–20483
39. Ch'en, F. F., Villafuerte, F. C., Swietach, P., Cobden, P. M., and Vaughan-Jones, R. D. (2008) *Br. J. Pharmacol.* **153,** 972–982
40. Boyarsky, G., Ganz, M. B., Sterzel, R. B., and Boron, W. F. (1988) *Am. J. Physiol.* **255,** C844–C856
41. Gillies, R. J., Liu, Z., and Bhujwalla, Z. (1994) *Am. J. Physiol.* **267,** C195–C203
42. Leem, C. H., and Vaughan-Jones, R. D. (1998) *J. Physiol.* **509,** 487–496
43. Carlsson, J., and Acker, H. (1988) *Int. J. Cancer* **42,** 715–720
44. Jones, D. T., Pugh, C. W., Wigfield, S., Stevens, M. F., and Harris, A. L. (2006) *Clin. Cancer Res.* **12,** 5384–5394
45. de Hemptinne, A., Marrannes, R., and Vanheel, B. (1987) *Can. J. Physiol. Pharmacol.* **65,** 970–977
46. Thomlinson, R. H., and Gray, L. H. (1955) *Br. J. Cancer* **9,** 539–549
47. Semenza, G. L. (2003) *Nat. Rev. Cancer.* **3,** 721–732
48. Mueller-Klieser, W. F., and Sutherland, R. M. (1982) *Br. J. Cancer* **45,** 256–264
49. Robey, I. F., Baggett, B. K., Kirkpatrick, N. D., Roe, D. J., Dosescu, J., Sloane, B. F., Hashim, A. I., Morse, D. L., Raghunand, N., Gatenby, R. A., and Gillies, R. J. (2009) *Cancer Res.* **69,** 2260–2268
50. McLachlan, E., Shao, Q., Wang, H. L., Langlois, S., and Laird, D. W. (2006) *Cancer Res.* **66,** 9886–9894
51. Svastová, E., Hulíková, A., Rafajová, M., Zat'ovicová, M., Gibadulinová, A., Casini, A., Cecchi, A., Scozzafava, A., Supuran, C. T., Pastorek, J., and Pastoreková, S. (2004) *FEBS Lett.* **577,** 439–445